Capillary zone electrophoresis of malto-oligosaccharides derivatized with 8-aminonaphthalene-1,3,6-trisulfonic acid

Claudia Chiesa and Csaba Horváth*

Department of Chemical Engineering, Yale University, New Haven, CT 06520 (USA)

ABSTRACT

Malto-oligosaccharides were derivatized via their reducing end with 8-aminonaphthalene-1,3,6-trisulfonic acid by reductive amination, and the separation and electrophoretic migration behavior of the labelled sugars were investigated by capillary zone electrophoresis. Series of linear malto-oligosaccharides were found particularly suitable for both the study of the effect of the operating conditions on the separation and the investigation of the relationship between the electrophoretic mobility and the molecular size of the homologues. The electrophoretic mobility of the malto-oligosaccharide conjugates was found to be a linear function of the molecular mass to the negative two-thirds power. The sugar derivatives employed here carry three negative charges due to the presence of the dissociated sulfonic acid groups even at strongly acidic pH. Therefore, the analytes can migrate in the electric field without interference by electroendosmotic flow and/or wall adsorption in uncoated silica capillaries at low pH. As a result, the separation of these carbohydrate conjugates can be carried out under such conditions with high speed and efficiency in free solution, *i.e.*, without an anticonvective medium such as a gel or a viscous polymer solution. Appropriate use of triethylammonium phosphate buffer, pH 2.5, as the background electrolyte improves not only the reproducibility, but also the efficiency and speed of the separation. The labelled sugars allow monitoring of the separation by UV detector or laser-induced fluorescence detector with concomitant enhancement of analytical sensitivity.

INTRODUCTION

The important role of complex carbohydrates in life processes is increasingly recognized. More and more therapeutic proteins produced by biotechnology entail glycan moieties that affect the biological activity, lifetime and specificity of the drug [1–3]. Consequently, there is a growing need for rapid analytical techniques of high resolution for oligosaccharides. However, the separation of carbohydrates is hampered by their similar chemical composition, as many oligosaccharides of biological interest consist of only a few kinds of residues and differ from each other mainly in their three-dimensional molecular structure. Moreover, the lack of chromophoric and/or fluorogenic functions in most sugar molecules impedes their high-sensitivity detection.

Traditionally, both chromatography and electrophoresis were employed for the analysis of carbohydrates. Most branches of chromatography such as size-exclusion, ion-exchange, ligand-exchange, reversed-phase and affinity chromatography as well as gas chromatography have found application in the quantitative and qualitative analysis of saccharides [4,5]. For complex oligosaccharides, the most popular HPLC method is anion-exchange chromatography at high pH with pulsed amperometric detection [6–8].

Electrophoresis of carbohydrates is encumbered by the absence of readily ionizable functions in most mono- and oligosaccharides. Whereas planar electrophoretic techniques have

---

* Corresponding author.

been widely used for the separation of naturally charged oligosaccharides and glycopeptides, the requirement of highly alkaline pH to ionize most carbohydrate molecules has impeded the use of electrophoresis for the separation of underivatized sugars. One approach to overcome this difficulty is the use of borate in the background electrolyte to form negatively charged borate complexes of neutral saccharides at moderately alkaline pH [9]. The borate complexes of carbohydrates are then separated by electrophoresis according to their differences in electric charge, molecular size and stability.

Polyacrylamide gel layers were preferentially employed for the electrophoretic separation of carbohydrate molecules. Since the diameter of the gel pores usually exceeded substantially the molecular dimensions of oligosaccharides and glycopeptides [10,11], their electrophoretic mobility in this matrix was largely determined by the charge-to-mass ratio, and molecular sieving did not contribute significantly to the separation. Despite its great merits, slab gel electrophoresis is a relatively slow process, and does not lend itself readily to automation or quantitative analysis with high precision.

In the past few years, capillary zone electrophoresis (CZE) has made great advances. This instrumental electrophoretic technique is particularly suitable for rapid analysis with high resolution as demonstrated by the analysis of peptide, protein and complex oligonucleotide mixtures [12–14]. A review of this technique can be found in the recent literature [15]. Moreover, CZE has been shown to also have promise for the analysis of mono- and oligosaccharides as well as glycoprotein fragments [16–20].

A promising approach in the CZE of carbohydrates entails their precolumn derivatization with reagents that contain ionogenic functions and suitable chromophoric or fluorogenic groups. Reductive amination at the reducing end of the saccharide with a reagent containing a primary amino group and allowing highly sensitive detection, offers a particularly convenient method for the preparation of these kinds of conjugates. Such a derivatization reaction of mono- and oligosaccharides with 2-aminopyridine was introduced originally for use in paper electrophoresis

and was later employed in HPLC [21]. It was recently modified for use in the CZE of monosaccharides and oligosaccharides as the borate complexes of their N-2-pyridylglycamine forms [22,23]. The separation by CZE of such malto-oligosaccharide conjugates was further improved by the addition of small amounts of tetrabutylammonium bromide to the background electrolyte at pH 5.0 [24]. In another example, reducing carbohydrates were derivatized with 3-(4-carboxybenzoyl)-2-quinolinecarboxaldehyde for the analysis by CZE with borate buffer in both free solution and highly concentrated polyacrylamide gel-filled capillaries [25–28]. With such derivatives, the use of polyacrylamide gel-filled capillaries was found to be essential for the CZE of carbohydrates at high resolution.

Most of the methods for the analysis of carbohydrates by CZE described so far in the literature are carried out at pH higher than 7.0, usually in order to form their borate complexes. Under such conditions, the silanol groups at the silica surface are dissociated and, as a result of the negatively charged capillary inner wall, considerable electroendosmotic flow is generated by the high electric field with possible untoward consequences for the separation. Furthermore, adsorption of positively charged analytes at the inner wall of the silica capillary significantly reduces the separation efficiency.

The goal of the present study was to investigate the potential of CZE in carbohydrate analysis under conditions where both electroendosmotic flow and adsorption at the capillary inner wall were negligible. This approach requires the use of derivatives which contain strongly acidic functions that dissociate even at low pH and facilitate UV and/or fluorescence detection. Derivatives of aromatic sulfonic acid can be particularly useful in this regard as they are ionized over a wide pH range. For this reason, reagents such as 7-aminonaphthalene-1,3-disulfonic acid and 8-amino-naphthalene-1,3,6-trisulfonic acid (ANTS), introduced for the derivatization of reducing saccharides prior to polyacrylamide slab gel electrophoresis, are potentially suitable also in CZE. Indeed, the reductive amination of N-acetylchitooligosaccharides with 7-amino-1,3-naphthalene disulfonic acid was recently de-

scribed for monitoring their chitinase-catalyzed hydrolysis by CZE analysis [16].

In our approach, we adapted the derivatization method with the fluorophore ANTS first described by Jackson and Williams [29,30] for use in polyacrylamide slab gel electrophoresis. The derivatization with ANTS imparts both electric charge and fluorescence to the saccharides. The three sulfonic acid groups in the ANTS moiety are negatively charged over a wide pH range and the concurrently high electrophoretic mobility of the derivatized carbohydrates facilitates their rapid separation. The ANTS derivatives can be used with UV detection and *a fortiori* with highly sensitive laser-induced fluorescence detection. Furthermore, ANTS, unlike other aminonaphthalene mono- and disulfonic acids, has adequate solubility in the reaction mixture [31] and is commercially available in a sufficiently pure form. Homologous malto-oligosaccharides of different provenance were selected as model substances because they span a wide molecular mass range. The mixtures were obtained from starch by acidic and/or enzymatic catalyzed hydrolysis and contained mainly linear homologues with up to approximately 40 glucose residues and a small amount of branched fragments.

EXPERIMENTAL

Equipment

A P/ACE Model 2100 capillary electrophoresis unit was used with System Gold Version 6.01 software (Beckman Instruments, Fullerton, CA, USA) and the 214-nm filter of the UV detector with a wavelength setting closest to the maximum absorbance wavelength for ANTS. Fused-silica capillary tubes of 365 μm O.D. with polyimide outer coating were obtained from Quadrex (New Haven, CT, USA) and employed without any coating of the inner wall. The dimensions of the capillaries used in the experiments were 270 mm × 50 μm, 370 mm × 50 μm and 670 mm × 20 μm. The pertinent migration distance from the inlet to the light beam of the detector, which passed through a narrow segment of the tube where the polyimide coating

was removed, was 70 mm shorter than the actual tube length.

Chemicals

Glucose (G1), maltose (G2), maltotriose (G3), maltotetraose (G4), maltopentaose (G5), maltohexaose (G6) and maltoheptaose (G7) standards as well as starch hydrolysate Cat. No. M3639 were purchased from Sigma (St. Louis, MO, USA). The main components of the latter mixture, referred to as mixture A, were linear malto-oligosaccharides of up to 12 glucose residues with a significant amount of branched isomers. Fig. 1 illustrates the structure of linear malto-oligosaccharides in which glucose molecules are joined by α-D(1,4) linkages. The number of glucose residues is denoted by "n" throughout this paper. Dextrin 15 (maltodextrin) starch hydrolysate was purchased from Fluka (Ronkonkoma, NY, USA). This sample, referred to as mixture B, contains over 30 linear malto-oligosaccharide homologues and only a small quantity of branched isomers. MALTRIN M040 (Maltodextrin) starch hydrolysate was a gift from Grain Processing (Muscatine, IA, USA). This sample contains linear malto-oligosaccharide homologues of up to almost 40 glucose residues and is referred to as mixture C. Sodium cyanoborohydride and mesityl oxide were purchased from Aldrich (Milwaukee, WI, USA). ANTS was obtained from Molecular Probes (Eugene, OR, USA). Dimethyl sulfoxide (DMSO) was purchased from Mallinckrodt (St.Louis, MO, USA), acrylamide was from Bio-Rad (Melville, NY, USA), and Triton X-100 was obtained from Rohm and Haas (Philadelphia, PA, USA). The buffers were prepared from
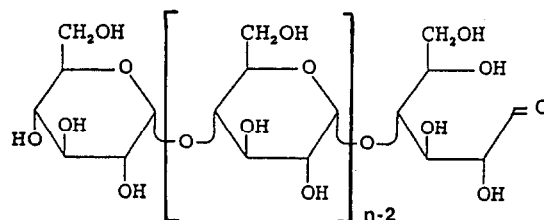

Fig. 1. General structure of linear malto-oligosaccharides: O - α - D - glucopyranosyl - (1 → 4) - [O - α - D - glucopyranosyl - (1 → 4)]$_{n-2}$-D-glucopyranose where n is the number of glucose residues in the molecule.

reagent grade phosphoric acid and sodium hydroxide supplied by Fisher Scientific (Pittsburgh, PA, USA) as well as triethylamine (TEA) purchased from Eastman Kodak (Rochester, NY, USA).

Derivatization with ANTS

The reductive amination of the saccharides with ANTS was adapted from the method described by Jackson [29]. In a typical procedure approximately 1 μmol of each authentic oligosaccharide standard with up to seven glucose units reacted in a microcentrifuge tube with 200 μl of 0.2 M ANTS solution in acetic acid–water (3:17, v/v) and 200 μl of 1 M NaCNBH$_3$ solution in dimethylsulfoxide. Furthermore, 20 μl of a 0.5 M aqueous solution of 1,3,5-benzene trisulfonic acid (BTA) were added to the reaction mixture to serve as a internal standard for the evaluation of the electropherograms. After mixing, the content of the tube was vortexed and then incubated for 15 h in a water bath at 40°C. Before the CZE injection, each sample was diluted twenty- to fortyfold with water and passed through 0.22-μm cellulose filters (Alltech, Deerfield, IL, USA). The average molecular mass of the starch hydrolysates was calculated for each mixture, and the conditions of the derivatization were optimized with regards to the amount of ANTS employed.

Electrophoresis

The samples were injected by applying 0.5 p.s.i. (1 p.s.i. = 6894.76 Pa) pressure for 3 to 7 s, and the approximate sample volumes were calculated according to the literature [32]. Electrokinetic injection was employed for the rapid separation depicted in Fig. 12. In most cases, the temperature was 25°C; only a few experiments were carried out at 50°C. Between runs, the capillary was flushed with approximately five tube-volumes of the background electrolyte. Some experiments were carried out with 30 and 50 mM phosphate buffers of pH 2.0 and 2.5, respectively, as the background electrolyte; the cathode was at the inlet end and the anode at the detector end of the capillary. In other experiments, 50 mM phosphate buffer, pH 9.0 or 9.4, was the background electrolyte, and the in-

strumental set up was configured so that sample introduction and detection took place at the anodic and cathodic ends, respectively. A mixture of 10 mM disodium phosphate and 10 mM trisodium borate, pH 9.4, was used in the study of the effect of borate on the electrophoretic mobility of the conjugated oligosaccharides. Electropherograms were obtained with a buffer prepared from a solution of 50 mM phosphoric acid and 10.8 mM TEA titrated with 1 M NaOH to pH 2.5. Major peaks in the electropherogram of the malto-oligosaccharides were identified by co-electrophoresis with ANTS derivatives of authentic standards containing up to seven glucose units.

Measurement of electroendosmotic flow

The magnitude of the electroendosmotic flow in capillaries filled with 50 mM phosphate buffer was determined from the migration times at 12 kV of three neutral tracers: acrylamide, mesityl oxide and Triton X-100. Subsequently, the electroendosmotic mobility was calculated and used to correct for the electrophoretic mobility when the ratio of the two mobilities was greater than 0.02.

In a particular set of experiments, the electroendosmotic flow velocity was measured by partially replacing sodium ions by TEA in the phosphate buffer, pH 2.5. Measurements were carried out using 50 mM phosphoric acid solutions containing 0, 3.6, 7.2, 10.8, 14.4, 21.6, 28.8 or 36 mM TEA that were titrated to pH 2.5 with 1 M NaOH. Before each measurement, the capillary was rinsed first with water and then with buffer each for 5 min. The electroendosmotic mobility was calculated with an average value from 3 measurements using phenol, DMSO and acrylamide as neutral markers.

### Experiments with laser-induced fluorescence detector

A capillary electrophoresis unit (P/ACE 2100) in the reversed polarity mode with the UV detector at 214 nm was used for the separation of malto-oligosaccharide mixture A with a 270 mm × 20 μm uncoated fused-silica capillary and 50 mM phosphate buffer, pH 2.5, at 25°C. The same sample was also separated with an *ad hoc*

capillary electrophoresis system consisting of a high-voltage power supply (Glassmann High Voltage, Whitehouse Station, NJ, USA) and a 20 μm I.D. uncoated capillary of 470 mm (minimum length required for system) without temperature control. Fluorescence excitation was accomplished using the 325-nm line of a helium–cadmium laser (2.8 mW, Liconix, Santa Clara, CA, USA). The beam was focused into the separation channel of a 20 μm I.D. fused-silica capillary using a plano convex lens [0.5 in. diameter (1 in. = 2.54 cm), 5 cm focal length, Oriel, Stratford, CT, USA]. Fluorescence originating from the illuminated section of the capillary separation channel was collected and collimated by a parabolic reflector. The collimated light from the reflector was directed through a series of two bandpass filters (520 nm, 3-cavity, Oriel) and detected by an end-on photomultiplier tube (PMT) (R374, Hamamatsu, Japan). The PMT output was converted to voltage using socket-mounted pre-amp assemblies (C1053, Hamamatsu) and electronically filtered (risetime = 1.0 s) using a home-made filter unit. The analog signal was digitized at 4 Hz using System Gold Software and a Model 406 analog-to-digital converter (Beckman Instruments). All laser-induced fluorescence detection (LIF) separations were performed at room temperature and samples were injected electrokinetically at typical conditions of 10 kV for 5 s.

RESULTS AND DISCUSSION

Derivatization of carbohydrates with ANTS

The derivatization reaction scheme is shown in Fig. 2. First, the reducing end of the saccharides reacts with the primary amino group of ANTS to form a Schiff base that is subsequently reduced to a secondary amine by sodium cyanoborohydride. According to Jackson [29], complete derivatization by ANTS occurs under optimal reaction conditions in 15 h as determined by using [14C]glucose; more than 99% of the glucose reacted. As monitored using glucose and/or maltose as model substances, complete derivatization could be achieved in less than 2 h when sodium cyanoborohydride was added to the
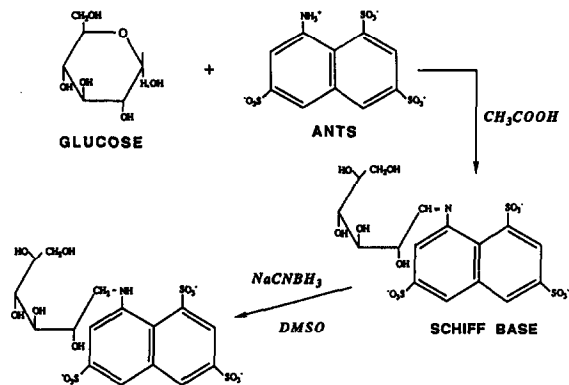
ANTS DERIVATIVE OF GLUCOSE

Fig. 2. Reaction scheme for the derivatization of carbohydrates with ANTS by reductive amination. The formula mass of the disodium salt of the ANTS–glucose conjugate (590) was used in the calculation of the molecular mass of the linear malto-oligosaccharide–ANTS conjugates with different number of glucose residues.

mixture at an advanced stage of the reaction and the temperature was increased from 40 to 80°C.

Another important aspect of the derivatization reaction is associated with the level of excess ANTS. Jackson routinely used approximately 200-fold excess of ANTS for the derivatization [29]. We have found that in the CZE of samples prepared with such a large excess of ANTS the peaks of the lower malto-oligosaccharides are masked by the large ANTS peak in the electropherogram. On the other hand, as suggested by Jackson [29], a fortyfold molar excess of ANTS sufficed for complete conversion, and under such conditions we observed no interference by excess ANTS in CZE.

The substantial advantage of ANTS as a labeling agent is that it is both a chromophore and a fluorophore which facilitates highly sensitive fluorescence detection of trace amounts under appropriate conditions. The UV spectrum of ANTS shows a maximum at approximately 220 nm followed by two other maxima at 270 and 360 nm; its molar adsorptivity in water is 5.700 cm^{-1} M^{-1} when measured at 360 nm. The spectrum of ANTS-derivatized maltose was found to be very similar except that the third maximum was shifted to 370 nm. With the UV detector, CZE analysis required relatively large amounts of sample with concomitant overload of

the system and reduced separation efficiency. When a 12-nl sample was subjected to CZE, approximately 15 fmol of ANTS-derivatized glucose could be detected at 214 nm (signal-to-noise ratio of 3) at the highest sensitivity setting.

As a fluorophore, ANTS has a maximum excitation wavelength at 360 nm in 50 mM phosphate buffer, pH 7.2, which shifts to 370 nm for the ANTS-derivatized maltose. The wavelength of maximum emission is at 515 nm. The fluorescent properties of ANTS facilitate LIF of its derivatives with a He–Cd laser with an output wavelength of 325 nm.

Fig. 3 depicts the results of some preliminary studies on the CZE of ANTS-derivatized malto-oligosaccharides from mixture A obtained by UV and LIF detection. The pattern is identical in both cases, but the sensitivity of LIF detection is about 3 orders of magnitude higher than that of the UV detection. As a result, a few attomoles can be analyzed by using an LIF detector. Moreover, as the capillary does not have to be overloaded, the potential of ANTS derivatization can be fully exploited without loss of efficiency. Precise values for the lower detection limit and for the efficiency of LIF detection are not available, but the preliminary results allow us to expect an efficiency of several hundred thousand theoretical plates per meter. In spite of the much higher sensitivity of LIF, the electropherogram depicted in Fig. 3B does not reveal
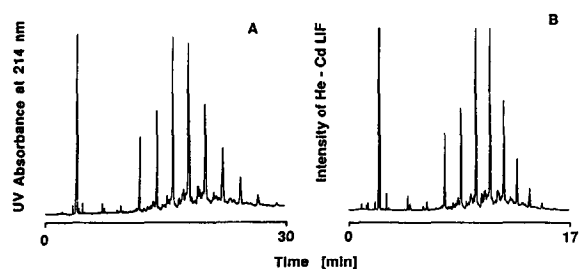

Fig. 3. Electropherograms of ANTS-derivatized malto-oligosaccharides (mixture A) obtained with UV and LIF detection. (A) 670 mm × 20 μm capillary; 200 mM phosphate buffer, pH 2.0; temperature, 25°C; voltage, 30 kV; UV detection at 214 nm; injected amount: 20 ng of ANTS-derivatized malto-oligosaccharide mixture. (B) 470 mm × 20 μm capillary; 200 mM phosphate buffer, pH 2.0; temperature, 25°C; voltage, 15 kV; He–Cd laser-induced fluorescence detector, emission wavelength 525 nm; injected amount: 70 pg of ANTS-derivatized malto-oligosaccharide mixture.

peaks that cannot be seen by UV detection at 214 nm. The derivatization reaction with ANTS appears to be a "clean" one not giving rise to minor side-products.

Theoretical aspects of CZE of carbohydrates derivatized with ANTS

Since the ANTS-derivatized saccharides are negatively charged over a wide pH range, they can be subjected to CZE at acidic pH where the electroendosmotic flow is usually negligible. Under such *arheic* (from the Greek *a* "without" and *rhéos* "flow") conditions, the sample components traverse the capillary in free solution solely by electrophoretic migration.

In the absence of electroendosmotic flow, the electrophoretic migration velocity u_{ep} is given by

$$u_{ep} = \mu_{ep}V/L \qquad (1)$$

where μ_{ep} is the electrophoretic mobility, and V is the potential across the capillary of length L [33,34].

Experimentally, the migration time t_m is measured and under arheic conditions given by

$$t_m = lL/\mu_{ep}V \qquad (2)$$

where L is the length of the capillary, and l is the pertinent migration distance, *i.e.* the tube length from the inlet to the detector's light beam.

In uncoated fused-silica capillaries of uniform surface properties at alkaline pH, the velocity of the electroendosmotic flow u_{eo} is expressed by

$$u_{eo} = \mu_{eo}V/L \qquad (3)$$

where μ_{eo} is the electroendosmotic mobility. Its magnitude depends [35] on the zeta potential, ζ, at the tube inner wall, the dielectric constant, ϵ, the viscosity of the fluid, η, and the permittivity of the vacuum, ϵ_0, as

$$\mu_{eo} = \epsilon_0\epsilon\zeta/\eta \qquad (4)$$

By using eqns. 2 and 4, we can estimate the value of the zeta potential from the migration time of neutral markers.

In the presence of electroendosmotic flow, the migration rates of charged molecules are de-

termined by both the pertinent electrophoretic mobilities and the magnitude of the electroendosmotic flow. The net migration velocity of a charged substance u is given by

$$u = u_{ep} + u_{eo} = (\mu_{ep} + \mu_{eo})V/L \qquad (5)$$

The sign of the electrophoretic and electroendosmotic mobility can be positive or negative according to the signs of the charge on the analyte molecule and those of the fixed charges at the tube inner wall.

According to eqns. 2 and 5, the observed migration time t_m is expressed by

$$t_m = lL/(\mu_{ep} + \mu_{eo})V \qquad (6)$$

The electrophoretic mobility is evaluated by the relationship

$$\mu_{ep} = (lL/V)[(1/t_m) - (1/t_0)] \qquad (7)$$

where t_0 is the measured migration time of a neutral marker.

In our case, the ANTS-derivatized saccharides bear a strong negative charge over the whole pH range under investigation. Therefore, we shall examine the three situations that follow. (a) At alkaline pH, the inner wall of silica capillaries is negatively charged so that the direction of the electrophoretic migration of negatively charged analytes is opposite to that of the electroendosmotic flow. In this case, the negatively charged sample components reach the detector at the cathodic end only if the absolute value of the electroendosmotic mobility is higher than that of the electrophoretic mobility. When the convective velocity is lower than the opposite electrophoretic migration velocity, the polarity of the electrodes must be reversed in order to detect the negatively charged sample components. (b) At strongly acidic pH, when the electroendosmotic flow is negligible, arheic or near-arheic separation conditions can be reached without anticonvective gel filling or coating of the tube inner wall. (c) Certain positively charged buffer components and additives, such as TEA, may be absorbed at the capillary inner wall so that it becomes positively charged. In this case, electroendosmotic flow takes place toward the anodic end of the capillary, i.e. in the direction

of the electrophoretic migration of the ANTS-derivatized saccharides.

CZE at high pH

Fig. 4 shows the electropherogram of ANTS-derivatized saccharides obtained in a fused-silica capillary with phosphate buffer, pH 9.0, and cathodic detection. Under alkaline conditions, the convective transport is faster than the electrophoretic migration of the components and the analytes are carried toward the cathode by electroendosmotic flow. The sample components appear at the detector in the order of increasing electrophoretic mobility. The migration times of the lower homologues, which have higher electrophoretic mobilities, are longer than those with a higher degree of polymerization; the lower homologues also exhibit broad and tailing peaks. Under the conditions used in Fig. 4, the ANTS peak does not appear in the electropherogram. ANTS has the highest charge-to-mass ratio among the sample components, and its migration rate in the opposite direction is greater than the electroendosmotic flow velocity. Therefore, it can only be detected anodically by reversing the polarity of the instrument. Fig. 4 also clearly
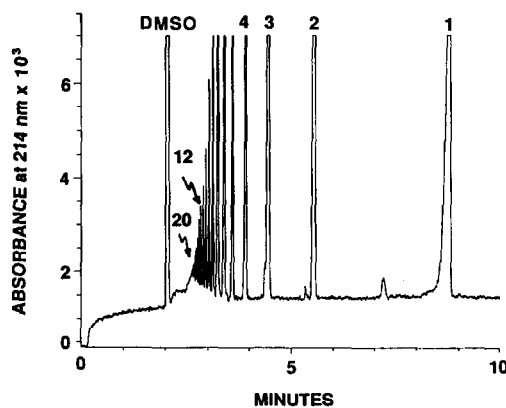

Fig. 4. Electropherogram of ANTS-derivatized malto-oligosaccharides obtained at alkaline pH in the presence of electroendosmotic flow with a fused-silica capillary, 370 mm × 50 μm. Conditions: 50 mM phosphate buffer, pH 9.0; temperature, 25°C; voltage, 17 kV; sample, 11 ng of mixture B derivatized with ANTS introduced at the anodic end. The number of glucose residues in the corresponding linear malto-oligosaccharide analytes, as determined by co-electrophoresis with authentic standards, is indicated for certain peaks.

illustrates that the electroendosmotic flow has an untoward effect on the separation; the migration times are not evenly spaced and the resolution decreases for homologues with increasing degree of polymerization. Therefore, for the resolution of the higher homologues it is desirable to carry out the separation of such samples with capillaries of commensurate dimensions in the absence of electroendosmotic flow.

CZE at low pH

As the magnitude of the electroendosmotic flow in silica capillaries depends on the pH of the medium, the appropriate pH for carrying out the separation under arheic conditions was experimentally determined over a wide pH range by measuring the migration time of neutral markers such as acrylamide, Triton X-100 and mesityl oxide, in 50 mM phosphate solutions as the background electrolyte. Upon plotting the electroendosmotic mobility against the pH (not shown), a kind of sigmoidal titration curve of the surface silanols is obtained with an inflection point around pH 5.3. As discussed in the literature [24,36–38], at low pH the ionization of the surface silanol groups is suppressed, and the electroendosmotic flow approaches zero. Indeed, at strongly acidic pH, the magnitude of the electroendosmotic mobility was often so low, i.e. less than $1.3 \cdot 10^{-9}$ m^{2}s^{-1}V^{-1}, that it did not affect the migration times of the ANTS conju-

gates. In contradistinction, under alkaline conditions the silanol groups are negatively charged and the electroendosmotic flow appears to reach a high plateau value. In such cases, the separation of ANTS derivatives could be carried out at or below pH 3.0 in the absence of appreciable electroendosmotic flow without treatment of the inner wall, use of an anticonvective medium or presence of additives in the background electrolyte. As a result, they could be separated rapidly by using a relatively simple electrophoretic system.

The electropherograms in Fig. 5 illustrate the separation of the ANTS-derivatized malto-oligosaccharides (mixture B) at pH 2.5 when the sample components traverse the tube solely by electrophoretic migration and can be detected anodically. The three sulfonic groups on the ANTS molecule impart strong negative charges and thus relatively high electrophoretic mobilities to the oligosaccharides. The use of phosphate buffer, pH 2.5, was appropriate because of its relatively high buffering power and low conductivity. Wall-adsorption of the highly negatively charged ANTS conjugates was negligible at pH 2.5, and the separation could be performed without such interference.

Since the net charge is the same for all derivatives, their migration velocity decreases with increasing number of glucose residues in the molecule. Indeed, short chain malto-oligosac-
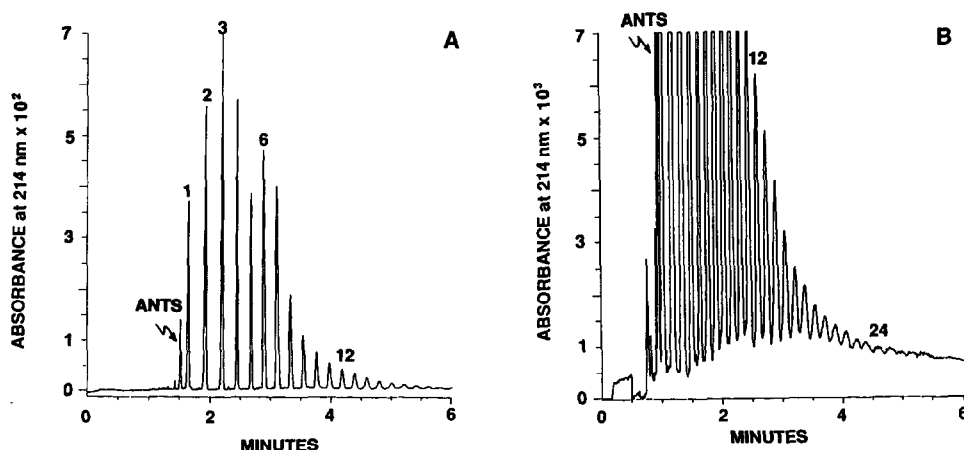

Fig. 5. Electropherograms of ANTS-derivatized malto-oligosaccharides (mixture B), obtained at acidic pH under arheic conditions at two different temperatures with a 270 mm × 50 μm capillary. (A) 50 mM phosphate buffer, pH 2.5; temperature, 25°C; voltage, 15 kV; 22 ng of sample. (B) 30 mM phosphate buffer, pH 2.5; temperature, 50°C; voltage, 17 kV; 31 ng of sample. In both cases, the samples were introduced at the cathodic end.

charides migrate faster than those containing a larger number of glucose residues as depicted in Fig. 5. The components of the mixture are very well resolved and baseline separation of more than 20 components was obtained contrary to the relatively poor separation of the higher homologues in the presence of electroendosmotic flow as shown in Fig. 4.

Comparison of Fig. 5A and B shows that separation of mixture B was improved and speed of analysis was increased by raising the temperature to 50°C. With increasing temperature, the viscosity of the liquid medium in the capillary decreases at a rate of approximately 2%/°C [39] leading to increased electrophoretic mobility. This enhancement of the transport properties accounts for the satisfactory separation of almost 30 homologues in 6 min.

The separation of the derivatized malto-oligosaccharide components of mixture A was also carried out under similar conditions, but a longer capillary tube of smaller inner diameter (670 mm × 20 μm) was needed for optimal resolution as illustrated by a typical electropherogram in Fig. 6. The main components were identified as the homologues of the linear malto-oligosaccharide series containing 4 to 12 glucose residues. The electropherogram shows a large number of small peaks that are attributed to branched isomers of the malto-oligosaccharides. This is further supported by the results of experiments in which mixture A was subjected to matrix-assisted laser desorption time-of-flight
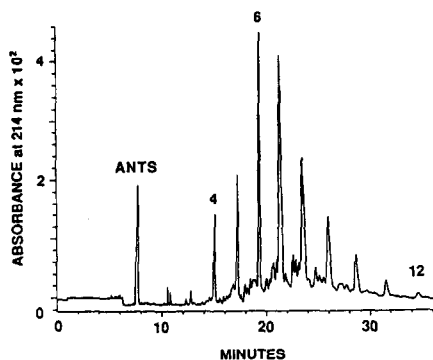

Fig. 6. Electropherogram of ANTS-derivatized malto-oligosaccharides (mixture A), obtained under arheic conditions. Capillary, 670 mm × 20 μm; 200 mM phosphate buffer, pH 2.0; temperature, 25°C; voltage, 30 kV; 100 ng of sample.

mass spectrometry (TOF-MS). The spectrum obtained by this highly sensitive technique revealed no components having molecular masses other than those of the linear malto-oligosaccharide homologues. The results in Fig. 6 confirm that oligosaccharide isomers can be separated with high resolution not only by reversed-phased HPLC [40,41], but also by CZE as ANTS conjugates. By using other derivatives, Nashabeh and El Rassi [18] have found that in the CZE of linear and branched oligosaccharides, the branched ones have longer migration times. Such a migration pattern is likely to apply in our case as well. In further investigations, samples of mixture B and C were used exclusively since they contain the highest number of readily identifiable linear homologues.

Relationship between electrophoretic mobility and molecular mass

The electrophoretic mobility of a molecule in free solution is, according to the simplest models [35,42], proportional to its electrical charge, q, and inversely proportional to the hydrodynamic radius, R. For small spherical ions in infinite conductive medium the electrophoretic mobility is expressed as

$$\mu_{ep} = q/6\pi\eta R \tag{8}$$

where η is the viscosity of the medium. If the model leading to eqn. 8 was applicable to our case involving linear malto-oligosaccharide–ANTS conjugates with molecular mass M_r, then $M_r^{1/3}$ could be substituted for R in eqn. 8, and plots of μ_{ep} against $M_r^{-1/3}$ would be linear. However, our experimental results do not show such linear dependence. Indeed, perusal of the literature on electrophoretic migration [35,42] reveals that the dependence of mobility on the molecular properties is quite complex and there is a lacuna for quantitative relationships between electrophoretic mobility, size and/or structure of large biological molecules despite considerable theoretical efforts over the last 30 years.

However, with the rapid development and growing applications of CZE, demand for such relationships is on the rise. For this reason, we investigated several approaches to correlate the electrophoretic mobilities of the ANTS-derivat-
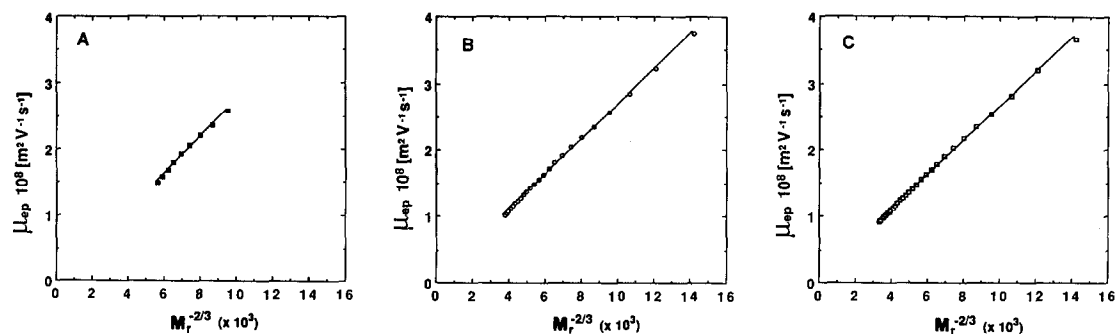
Fig. 7. Plot of the electrophoretic mobility of ANTS-derivatized malto-oligosaccharide homologues against their molecular mass to the $-2/3$ power. (A), (B) and (C) show data obtained with mixtures A, B and C, respectively. Capillary, 270 mm × 50 μm; 50 mM phosphate buffer, pH 2.5; temperature, 25°C; voltage, 17 kV.

ized malto- oligosaccharides with their molecular size. Such homologues carry the same electric charge and differ only in the number of glucose residues, and therefore they should represent a simpler system than other biopolymers such as peptides and nucleic acids. Peptide mobilities in paper electrophoresis have been successfully correlated to the molecular mass by Offord [43] using the relationship

$$\mu_{ep} = Cq(M_r)^{-2/3} \qquad (9)$$

where C is a constant. Eqn. 9 has some theoretical support for rodlike molecules whose mobility depends on molecular surface area rather than on radius.

We have evaluated the electrophoretic mobilities of ANTS–malto-oligosaccharides under conditions given in Fig. 5A at three different voltage settings (15, 17 and 20 kV). The highly reproducible results showed that the mobilities were independent of the electric field strength in agreement with theoretical prediction, indicating that the system was well behaving and electroendosmotic flow was indeed negligible. The data were plotted against $M_r^{-2/3}$ and the results are illustrated in Fig. 7. As seen, the plots show excellent linearity for all three malto-oligosaccharide mixtures. The mobility–molecular mass relationship represented by eqn. 9 was also successfully used by Wenn [44] for dansyl-glycopeptides with glycan moieties having different numbers of monosaccharide residues. Both series are composed of rather uniform monosaccharide residues, and magnitude and terminal

location of the charges carried by each member of the series are the same. It appears that in such relatively simple cases, eqn. 9 offers useful mobility–molecular size relationships also in the electrophoresis of ANTS derivatives of various oligosaccharides with biological significance. This possibility may further expand the usefulness of ANTS as a fluorescent marker which facilitates high sensitivity detection.

Other linear relationships between the number of glucose residues in the malto-oligosaccharides and their migration time or electrophoretic mobilities have also been found; they are shown in Fig. 8. The migration time depends linearly on the number of glucose units as seen in Fig. 8A.
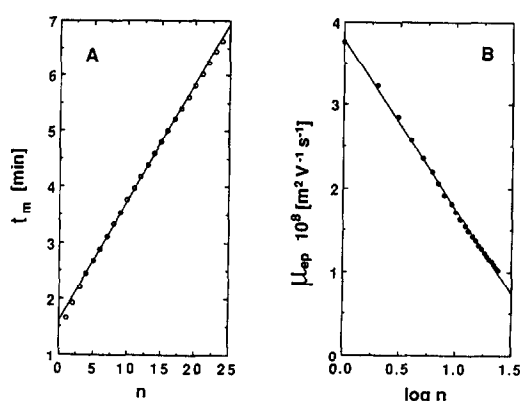

Fig. 8. Plots illustrating the dependence of electrophoretic properties of ANTS-derivatized malto-oligosaccharide homologues on the number of glucose residues. (A) Plot of the electrophoretic migration time against the number of glucose residues. (B) Plot of the electrophoretic mobility against the logarithmic number of glucose units in the molecule. Experimental conditions as in Fig. 5A.

Such linear relationships between t_m and the number of residues have been observed with oligomers in gel electrophoresis, *i.e.* under arheic conditions, in the following two cases: firstly, when the series of molecules under investigation have the same electrical charge and differ only in the number of neutral residues as with malto-oligosaccharide–ANTS conjugates, and secondly, when both the charge and molecular size increase in equal increments as is the case with oligonucleotides. Another empirical quasi-linear relationship is shown in Fig. 8B between the electrophoretic mobility of linear malto-oligosaccharide–ANTS conjugates and the logarithmic number of glucose residues. This correlation has been found convenient in this study among others for identification of the peaks in the electropherograms. The use of homologues offers a convenient means of testing the electrophoretic system in light of these linear relationships. However, further investigations are required to elucidate their basis at the molecular level.

The use of the linear relationships is further illustrated in Fig. 9 by plots of different sets of electrophoretic mobilities evaluated under diverse conditions. In one case, the electrophoretic mobility of the derivatized malto-oligosaccharide homologues was obtained directly from arheic migration times at pH 2.5 by eqn. 2. In the

other, the electrophoretic mobility was calculated according to eqn. 5 from data measured in phosphate buffer at pH 9.4 with correction for the effect of the electroendosmotic flow on the overall migration rates. In the third case, the electrophoretic mobilities were evaluated from data measured at pH 9.4 in 10 mM phosphate buffers containing 10 mM borate. Measuring in the absence of electroendosmotic flow at pH 2.5 and calculating from the two sets of data obtained in the presence of strong electroendosmotic flow at pH 9.4, the electrophoretic mobilities show excellent linear correlation. The results are not unexpected since the three sulfonic acid functions are fully dissociated at either pH. Nevertheless, this finding also suggests that no significant changes occurred in the viscosity of the electrophoretic medium or in the relevant hydrodynamic size parameter of the sample molecules upon changing from pH 2.5 to 9.4. The higher electrophoretic mobility of the malto-oligosaccharides when borate is added to the buffer solution is readily explained by the formation of negatively charged complexes between borate and certain sugars at sufficiently high pH [38]. Such complexation augments the negative charge on the analytes and thus accounts for the relatively high electrophoretic mobility. The slope of the straight line for the mobilities measured in the presence of borate is steeper than for those obtained in its absence as seen in Fig. 9. Evidently, with increasing size of the carbohydrate moiety, the negative charge on the analyte molecules also increases due to borate complexation. The effect of the incremental charge on the electrophoretic mobility is greater than the opposing influence of the higher molecular mass of the borate complexes.

Effects of the addition of TEA to the background electrolyte

The electropherograms in Figs. 5A and 5B demonstrate that ANTS-derivatized malto-oligosaccharides can be efficiently and rapidly separated using untreated silica capillaries in free solution at low pH with a relatively simple electrophoretic system. Nonetheless, it is important to emphasize that when uncoated fused-silica capillaries are used, the reproducibility of the results usually depends on the uniformity and
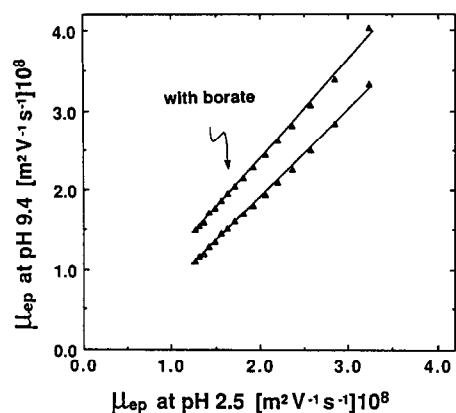
Fig. 9. Correlation between electrophoretic mobilities directly observed at pH 2.5 and calculated from data measured at pH 9.4 with malto-oligosaccharide–ANTS conjugates in the presence (▲) and absence (△) of 10 mM borate buffer. Capillary, 370 mm × 50 μm; 50 mM phosphate buffer; temperature 25°C; voltage, 17 kV.

constancy of surface properties. In practice, the inner surface of silica capillaries varies even within the same batch of material; this, together with differences in the history of the capillary, give rise to variations in the magnitude of the electroendosmotic flow particularly in the pH range from 4.0–10. It is therefore essential to establish a rigorous washing protocol that allows one to equalize the different surface properties of importance and thus facilitate reproducible measurements as recommended by Schwer and Kenndler [36]. Considering the possibilities of a significant interaction between the phosphate ions and the silanol groups at the tube inner wall [45], we maintained the phosphate level constant in the solutions used in the washing procedure. We found that the respective use of 1 M trisodium phosphate and 1 M phosphoric acid solutions in the alkaline and acidic washing steps palpably enhanced the reproducibility of measurements.

In order to improve further the reproducibility and efficiency of the analytical procedure, TEA (widely employed in reversed-phase chromatography as a masking agent for the silanol groups at the stationary phase surface [46]), was added to the background electrolyte. Indeed, the use of the above washing protocol and of TEA in the sodium phosphate buffer resulted in satisfactory reproducibility; the relative standard deviation in the migration times of the ANTS conjugates of the malto-oligosaccharides in mixture B from 20 consecutive injections into two different capillaries was better than one percent. In general, higher efficiency also manifested itself in sharp and symmetrical peaks. Moreover, triethylammonium ions have relatively low mobility and therefore allow the employment of high voltage in order to bring about high-speed separations without the untoward effects of high current.

Most striking was the observation that varying the relative concentration of triethylammonium and sodium ions in phosphate buffer at pH 2.5 we could modulate the zeta potential at the inner surface of the capillary in a reproducible fashion. Typical results are shown in Fig. 10. The value for the zeta potential was calculated from the observed electroendosmotic flow velocity according to eqn. 4. Increasing the TEA concentration in the phosphate buffer as the percentage of the
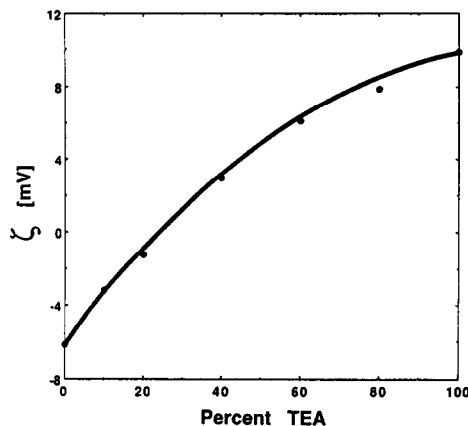

Fig. 10. Zeta potential titration curve of a 270 mm × 50 μm fused-silica capillary with triethylamine in 50 mM sodium phosphate buffer, pH 2.5, at 25°C. The abscissa is the triethylammonium ion (TEA$^+$) concentration as the percentage of the total cation (TEA$^+$ and Na$^+$) concentration. Electroendosmotic velocity was measured with phenol and acrylamide as indicators.

total cation concentration strengthens the interaction of the amine with the inner surface of the capillary and brings about a progressive decrease in the negative charge at the wall. In the case illustrated, when the fraction of TEA reaches about 25% of the total cationic concentration, the "point of zero zeta potential" is reached, and the electroendosmotic flow becomes negligibly small. Difficulties beset accurate determination of the point of zero charge because of the problems associated with the measurement of very low electroendosmotic flows. As inconsistencies in the inner surface of different capillaries were observed, different concentrations of TEA might be required in order to reach the zero point. Nevertheless, establishing a narrow range of TEA concentration that permits operation in the absence of appreciable electroendosmotic flow, *i.e.* under arheic conditions, is possible. This finding does not contradict the earlier observations that arheic conditions were also obtained without addition of TEA to the phosphate buffer at pH 2.5. It should be noted that with certain capillary tubes of different provenance and/or history arheic conditions were not always reached even by using phosphate buffer, pH 2.5, alone, and the reproducibility of those results was often not satisfactory. In contrast, the proper use of TEA additive with phosphate

buffer of pH 2.5–3.0 not only yields high speed and efficiency of the separation but also allows us to modulate the properties of the capillary inner wall to obtain a desired value of the electroendosmotic flow. Fig. 11A illustrates the separation of malto-oligosaccharide mixture C in free solution using sodium triethylammonium phosphate buffer, pH 2.5, under arheic conditions. Comparison of the results in Fig. 11A to those in Fig. 5A shows a significant increase in the speed of analysis without loss of separating efficiency for the higher members of the homologous series.

The effect of TEA is attributed to its interaction with the capillary inner wall rather than an interaction between the negatively charged ANTS derivatives and the triethylammonium ions. This is supported by the observation that at various TEA concentrations up to 36 mM in the phosphate buffer, the electrophoretic mobilities of the homologues were essentially constant; only a slight change in the electrophoretic mobilities of the lowest homologues was noted. On the other hand, in preliminary experiments with various alkyl diamines and triamines as buffer additives, a dramatic increase in the electrophoretic migration times was observed. This effect is likely to be associated with a strong interaction between such amines and the ANTS derivatives which alters the effective charge on the analyte molecules.

The zeta potential titration curve in Fig. 10 also shows that increasing the concentration of TEA in the buffer above approximately 25% of the total cationic concentration progressively imparts positive charge to the inner wall of the capillary in agreement with recent observations by others [47]. As a consequence, electroendosmotic flow toward the anodic end of the capillary is generated when the voltage is applied. Since the electrophoretic migration of the strongly negatively charged ANTS derivatives takes place in the same direction, the electroendosmotic flow at a sufficiently high TEA concentration has the beneficial effect of enhancing the speed of separation. Under such conditions, when both electroendosmotic flow and electrophoretic migration occur toward the detector end, the separation of more than 20 homologues can be carried out in less than 3 min, as shown in Fig. 11B. This approach permits a dramatic reduction of the analysis time for less complex samples; an example of ultrafast separations is illustrated in Fig. 12 where three short-chain malto-oligosaccharides are resolved in less than 10 s.

Electrophoretic behavior of derivatized saccharides in free solution and in polyacrylamide gels

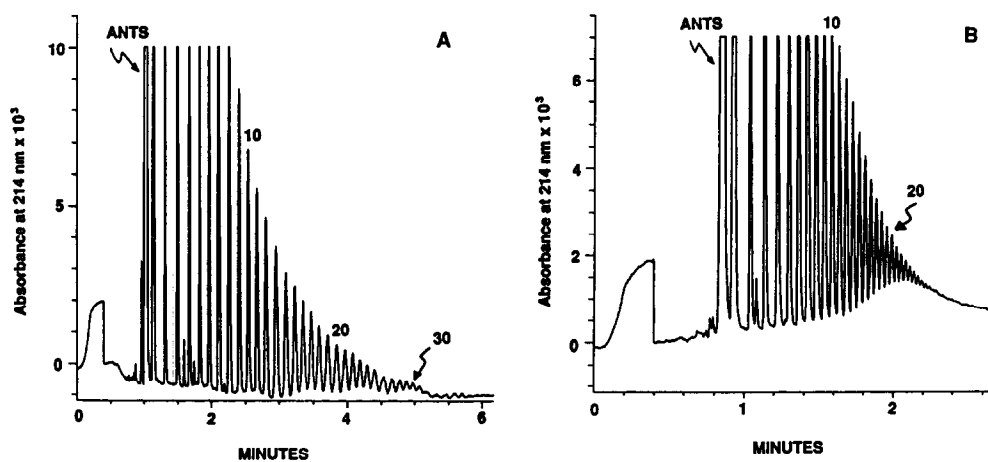As exemplified by the results in Figs. 5A, 11A, 11B, and 13, the derivatization of malto-

Fig. 11. Electropherogram of ANTS-derivatized malto-oligosaccharides (mixture C) obtained (A) with 50 mM sodium/triethylammonium phosphate buffer, pH 2.5, containing 10.8 mM TEA, (B) with 50 mM triethylammonium phosphate, pH 2.5. In both cases: capillary, 270 mm × 50 μm; temperature, 25°C; voltage, 22 kV; 80 ng of sample.
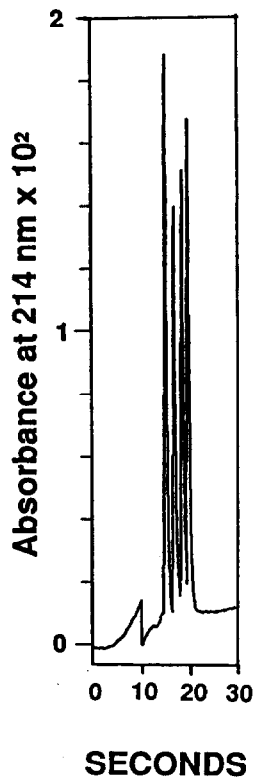
Fig. 12. Rapid separation of ANTS-derivatized malto-oligosaccharides. Conditions as in Fig. 11B, except for temperature of 50°C. Sample components in order of appearance: ANTS, ANTS-derivatized maltose, ANTS-derivatized maltotetraose, ANTS-derivatized maltohexaose.
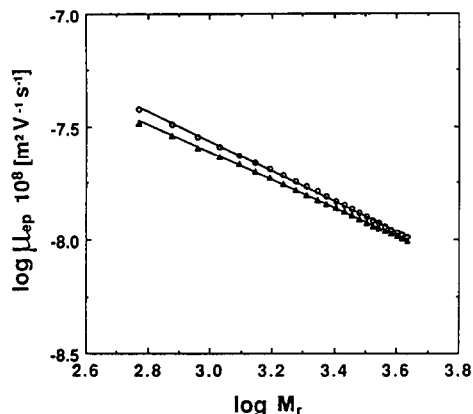
Fig. 13. Double logarithmic plots of the electrophoretic mobility of ANTS-derivatized malto-oligosaccharides against their molecular mass. Data were measured with 50 mM sodium phosphate buffer, pH 2.5 (O), and 50 mM tri-ethylammonium phosphate buffer, pH 2.5 (▲). Capillary, 270 mm × 50 μm; temperature, 25°C; voltage, 17 kV.

oligosaccharides with ANTS allows arheic separation of a very wide range of such homologues with excellent resolution in untreated fused-silica capillaries. According to the literature [25–28], however, the use of polyacrylamide gel-filled capillaries is essential for the CZE of complex mixtures of large oligosaccharides with fluorescent markers other than ANTS. This prompted us to investigate whether a sieving effect that may be associated with the use of a highly concentrated cross-linked polyacrylamide gel in the capillary or in the slab configuration would indeed provide higher selectivity for the separation.

We examined three different systems: (a) ANTS-derivatized saccharides, separated in polyacrylamide gel slab by Jackson [29], (b) ANTS-derivatized malto-oligosaccharides, separated in free solution at pH 2.5 in the present study and (c) 3-(4-carboxybenzoyl)-2-quinoline-carboxaldehyde (CBQCA)-derivatized malto-oligosaccharides, separated in capillaries filled with highly concentrated polyacrylamide gel by Liu et al. [25]. The selectivity of each of the three systems was evaluated by plotting the ratio of the electrophoretic mobilities of two neighboring homologues, μ_n/μ_{n+1}, against the number of glucose residues. As seen in Fig. 14A, the presence of the gel does not enhance the relative electrophoretic mobilities of oligosaccharide derivatives containing at least up to 20 glucose residues and the difference in the labels used in systems (b) and (c) also has no major effect on the selectivity. For comparison, the dependence of the relative electrophoretic mobility on the reciprocal of the corresponding molecular mass ratio to the 2/3 power is also shown in Fig. 14A. In agreement with the results illustrated in Fig. 7A and B, the change in the relative electrophoretic mobility of the malto-oligosaccharide conjugates with the molecular size over a wide molecular mass range is well represented by this relationship. Indeed, plots of log μ_{ep} against log M_r were linear with slopes of -0.63, -0.60, and -0.56 according to the data obtained in free solution, in gel-filled capillaries and in slab gel, respectively.

The electrophoretic mobilities of ANTS-derivatized malto-oligosaccharides in free solution
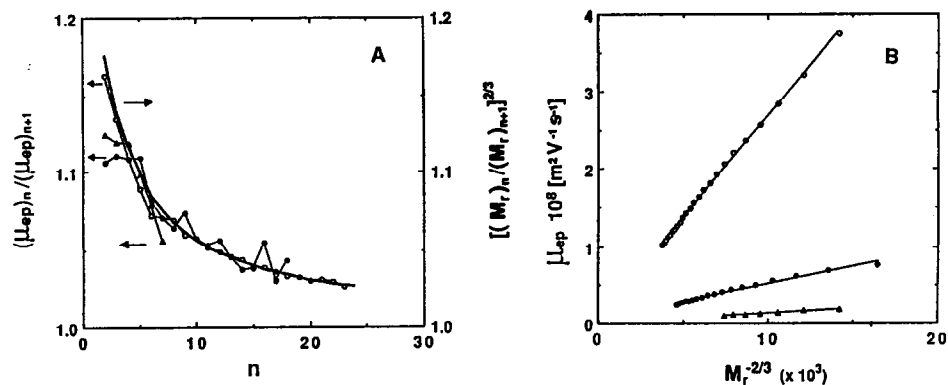
Fig. 14. Illustration of the electrophoretic behavior of malto-oligosaccharide conjugates in three different systems: ANTS derivatives in free solution CZE under arheic conditions (O) (see Fig. 5A), ANTS derivatives in slab gel electrophoresis (▲) [25], and CBQCA derivatives in polyacrylamide gel filled capillaries (●) [30]. The formula mass of the CBQCA–glucose conjugate (474) was used in the calculation of the molecular masses of the homologues. (A) Plots of the relative electrophoretic mobility of the conjugated oligosaccharides on the number of glucose residues. The solid line represents the plot of the molecular mass ratio to the two third power of the neighboring homologues as a function of the number of glucose residues. (B) Dependence of the electrophoretic mobility on the molecular mass to the $-2/3$ power.

at low pH can be compared to the electrophoretic mobilities of CBQCA-derivatized malto-oligosaccharides in gel-filled capillaries by the plots of μ_{ep} against $M_r^{-2/3}$ in Fig. 14B. The slopes of the two pertinent straight lines in Fig. 14B suggest that the electrophoretic mobilities of ANTS derivatives are higher by a factor of about 6 than those of the CBQCA derivatives. Much of this difference can be attributed to differences in the charges carried by the two label-moieties: ANTS and CBQCA. Whereas ANTS-derivatized saccharides have three negative charges, the dissociation of the carboxylic group in CBQCA derivatives results in only a single negative charge. However, the negative charge is believed to increase with the molecular size of the oligosaccharide moiety due to the formation of borate complexes under the operating conditions which results in higher electrophoretic mobilities [25]. From the comparison of the slopes, we can infer that the electrophoretic migration rates of derivatized malto-oligosaccharides ($n < 40$) are at least two times lower in the gel present in the capillary than in free solution. Fig. 14B also shows a plot of the electrophoretic mobilities of ANTS-derivatized oligosaccharides in polyacrylamide gel slab as estimated from the data by Jackson [29] against $M_r^{-2/3}$. This allows a direct

comparison, though limited to the first seven components of the homologous series, of the electrophoretic mobilities of ANTS derivatives in free solution and in the polyacrylamide gel slab. From the data shown in Fig. 14B, the mobility of the ANTS derivatives appears to be lower by a factor of 22 in the cross-linked gel than in free solution. The relatively high electrophoretic mobilities of the derivatized oligosaccharides under the conditions described in this study are mainly responsible for the high speed of analysis without the loss of resolution.

ACKNOWLEDGEMENTS

and Professor P.G. Righetti for their support and helpful discussions.

REFERENCES

1 N. Sharon, Complex Carbohydrates: Their Chemistry, Biosynthesis and Functions, Addison-Wesley, Reading, MA, 1975, pp. 33–47.
2 R. Montgomery, in W. Pigman and D. Horton (Editors), The Carbohydrates, Vol. 26, Academic Press, New York, 2nd ed., 1970, pp. 677–696.
3 N. Sharon, Trends Biochem. Sci., 9 (1984) 198.
4 S.C. Churms, J. Chromatogr., 500 (1990) 555.
5 M.F. Chaplin and J.F. Kennedy (Editors), Carbohydrate Analysis: A Practical Approach, IRL Press, Oxford, 1986, pp. 43–51.
6 S. Hughes and D.C. Johnson, Anal. Chim. Acta, 132 (1981) 11.
7 S. Hughes and D.C. Johnson, J. Agric. Food Chem., 30 (1982) 712.
8 L.J. Basa and M.W. Spellman, J. Chromatogr., 499 (1990) 205.
9 A.B. Foster, Adv. Carbohydr. Chem., 12 (1957) 81.
10 O. Prem Das and E.J. Henderson, Anal. Biochem., 158 (1986) 390.
11 S. Weitzman, V. Scott and K. Keegstra, Anal. Biochem., 97 (1979) 438.
12 A.S. Cohen and B.L. Karger, J. Chromatogr., 397 (1987) 409.
13 A.S. Cohen, D. Najarian, J.A. Smith and B.L. Karger, J. Chromatogr., 458 (1988) 323.
14 A.S. Cohen, S. Terabe, J.A. Smith and B.L. Karger, Anal. Chem., 59 (1987) 1021.
15 W.G. Kuhr and C.A. Monnig, Anal. Chem., 64 (1992) 389R–407R.
16 K.B. Lee, A. Al-Hakim, D. Loganathan and R.J. Linhardt, Carbohydr. Res., 214 (1991) 155.
17 P.J. Oefner, A.E. Vorndran, E. Grill, C. Huber and G.K. Bonn, Chromotagraphia, 23 (1992) 308.
18 W. Nashabeh and Z. El Rassi, J. Chromatogr., 600 (1992) 279.
19 P.M. Rudd, I.G. Scragg, E. Coghill and R.A. Dwek, Glycocong. J., 8 (1992) 86.
20 M. Taverne, A. Rainet, D. Biou, M. Sclüter, R. Werner and D. Ferrier, Electrophoresis, 13 (1992) 358.
21 N. Tomiya, J. Awaya, M. Kurono, S. Endo, Y. Arata and N. Takahashi, Anal. Biochem., 171 (1988) 73.
22 S. Honda, A. Makino, S. Suzuki, and K. Kakeki, Anal. Biochem., 191 (1990) 228.
23 S. Honda, S. Iwase, A. Makino and S. Fujiwara, Anal. Biochem., 176 (1990) 72.
24 W. Nashabeh and Z. El Rassi, J. Chromatogr., 514 (1990) 57.
25 J. Liu, O. Shirota and M.N. Novotny, J. Chromatogr., 559 (1991) 223.
26 J. Liu, O. Shirota, D. Wiesler and M.N. Novotny, Proc. Natl. Acad. Sci. U.S.A., 88 (1991) 2302.
27 J. Liu, Y.Z. Hsieh, D. Wiesler and M.N. Novotny, Anal. Chem., 63 (1991) 408.
28 J. Liu, O. Shirota and M.V. Novotny, Anal. Chem., 64 (1992) 973.
29 P. Jackson, Biochem. J., 270 (1990) 705.
30 P. Jackson and G.R. Williams, Electrophoresis, 12 (1991) 94.
31 R.J. Stack and M.T. Sullivan, Glycobiology, 2 (1992) 85.
32 R.S. Rush and B.L. Karger, Sample injection with PIACE System 200: Importance of Temperature Control with Respect to Quantitation; Technical Bulletin TIBC-104, Beckman Instruments, Spinco Division, Palo Alto, CA, 1990.
33 F.E.P. Mikkers, F.M. Everaerts and Th.P.E.M. Verheggen, J. Chromatogr., 169 (1979) 11.
34 J.W. Jorgenson and K.D. Lukacs, J. Chromatogr., 218 (1981) 209.
35 P.C. Hiemenz, Principles of Colloidal and Surface Chemistry, Marcel Dekker, New York, 2nd ed., 1986, p. 751.
36 C. Schwer and E. Kenndler, Anal. Chem., 63 (1991) 1801.
37 C. Schwer and E. Kenndler, Chromatographia, 30 (1990) 546.
38 S. Hoffstetter-Kuhn, A. Paulus, E. Gassmann and H.M. Widmer, Anal. Chem., 63 (1991) 1541.
39 J. Harbaugh, M. Collette and H.E. Schwartz, Determination of Injection Volumes with PIACE System 200; Technical Bulletin TIBC-103, Beckman Instruments, Spinco Division, Palo Alto, CA, 1990.
40 V.M.B. Cabalda, J.F. Kennedy and K. Jumel, in R.B. Friedman (Editor), Biotechnology of Amylodextrin Oligosaccharides (ACS Symposium series, No. 458), American Chemical Society, Washington, DC, 1991, pp 140–170.
41 R.N. Ammeraal, G.A. Delgado, F.L. Tenbarge and R.B. Friedman, Carbohydr. Res., 215 (1991) 179.
42 H. Mueller, in E.J. Cohn and J.T. Edsall (Editors), Proteins, Amino Acids and Peptides, Reinhold, New York, 1943, Ch. 25, pp. 623–643.
43 R.E. Offord, Nature, 211 (1966) 591.
44 R.V. Wenn, Biochem. J., 145 (1975) 281.
45 B.M. Mitsyuk, Russ. J. Inorg. Chem., 17 (1972) 471.
46 K.E. Bij, Cs. Horváth, W.R. Melander and A. Nahum, J. Chromatogr., 203 (1981) 65.
47 W.R. Jones, P. Jandik and M. Merion, U.S. Pat., 5 104 506 (1992).